Polymerization of Tubulin In Vivo: Direct Evidence for Assembly onto Microtubule Ends and from Centrosomes

BOHDAN J. SOLTYS and GARY G. BORISY
Laboratory of Molecular Biology, University of Wisconsin, Madison, Wisconsin 53706

ABSTRACT Microtubule assembly in vivo was studied by hapten-mediated immunocytochemistry. Tubulin was derivatized with dichlorotriazinylaminofluorescein (DTAF) and microinjected into living, interphase mammalian cells. Sites of incorporation were determined at the level of individual microtubules by double-label immunofluorescence. The haptenized tubulin was localized by an anti-fluorescein antibody and a second antibody conjugated with fluorescein. Total microtubules were identified by anti-tubulin and a secondary antibody conjugated with rhodamine. Contrary to recent studies (Salmon, E. D., et al., 1984, *J. Cell Biol.*, 99:2165–2174; Saxton, W. M., et al., 1984, *J. Cell Biol.*, 99:2175–2186) which suggest that tubulin incorporates all along the length of microtubules in vivo, we found that microtubule assembly in interphase cells was in vivo, as in vitro, an end-mediated process. Microtubules that radiated out toward the cell periphery incorporated the DTAF-tubulin solely at their distal, that is, their plus ends. We also found that a proportion of the microtubules connected to the centrosomes incorporated the DTAF-tubulin along their entire length, which suggests that the centrosome can nucleate the formation of new microtubules.

How do microtubules grow and shorten in living cells? How do they exchange subunits in the steady-state? A determination of whether the addition and loss of subunits occur along the length of the microtubule or are restricted to its ends would be fundamental to our understanding of microtubule dynamics in vivo.

Microtubule dynamics have been analyzed in vitro with purified proteins and reconstitution systems, and the results are clear. In vitro, microtubules grow and shorten by addition and loss of subunits at their ends (1). Treadmilling, which occurs in the steady-state (2), results from the differential rates of addition and loss at the ends (3). The recently proposed model of dynamic instability (4) is also an end-mediated process. However, the in vitro studies cannot, by their nature, provide the answer for living cells. Intriguingly, efforts to study microtubule dynamics in vivo have led to different conclusions.

Observations of the mitotic spindle made with polarized light microscopy (5, 6) led Inoué to propose that the reaction mechanism could be represented as a phase transition between two states, A $\rightleftharpoons$ B, where A denotes oriented material (microtubules) and B, nonoriented material (tubulin subunits). The microtubule was viewed as a special type of cylindrical micelle and would grow or shorten by subunits entering or exiting the micelle. A hallmark of this mechanism is that exchange of subunits between the polymer and the solution would occur all along the length of the polymer and would not be restricted to its ends.

Recent observations by use of fluorescently derivatized tubulin have supported this conclusion (7, 8). Cells microinjected with fluorescent tubulin showed patterns of incorporation that were apparently uniform throughout the microtubule network. Analysis of fluorescence recovery after photobleaching also showed apparently uniform recovery. These observations were interpreted as being most compatible with exchange along the length of a microtubule. The exchange could occur by some form of lattice breathing and intercalation of subunits or, perhaps, by rapid breaking and reannealing (7). The disparity between these conclusions and those drawn from the in vitro results presents a paradox.

In this paper, we report results on the mechanism of microtubule growth in vivo in interphase mammalian cells. Our approach differs from previous ones in that we have attempted to resolve events at the level of single microtubules rather

THE JOURNAL OF CELL BIOLOGY · VOLUME 100 MAY 1985 1682-1689

than at the level of populations of microtubules, as has been done in the studies that use birefringence measurement (5, 6) or direct fluorescence emission and fluorescence recovery after photobleaching (7, 8). We used the approach of microinjection and hapten-mediated immunocytochemistry (9, 10, 11) to determine the pattern of incorporation of haptenized tubulin. Our results show that microtubules in interphase mammalian cells do not incorporate subunits along their length. Rather, they grow in vivo as in vitro by addition of subunits preferentially at their plus ends. In addition, we present evidence for nucleation of microtubules from the centrosome.

MATERIALS AND METHODS

Preparation of Dichlorotriazinylaminofluorescein-Tubulin: Microtubule protein was prepared from porcine brain by cycles of assembly and disassembly (12). Pure tubulin was prepared from the microtubule protein by DEAE cellulose column chromatography (13). Dichlorotriazinylaminofluorescein (DTAF)[1] was synthesized as has been described (14). Pure tubulin at 7–8 mg/ml was polymerized into microtubules at 37°C in 5% dimethyl sulfoxide (DMSO) in 100 mM PIPES, pH 6.94, 0.1 mM $MgCl_2$, 1 mM GTP. DTAF dissolved in DMSO was mixed in rapidly at a final reagent-to-tubulin ratio of 20:1 (final DMSO concentration, 10%). After 15 min at 37°C, microtubules were sedimented, depolymerized at 0°C, and purified by two cycles of polymerization at 37°C in 10% DMSO and depolymerization at 0°C in the absence of DMSO with differential centrifugation (12). The assembly properties of the DTAF–tubulin were normal by the criteria of temperature dependence of polymerization and electron microscopic morphology. Final protein yield was ~50% with a fluorochrome-to-tubulin ratio of 0.5 based on an absorption coefficient of 6.3×10^4 M^{-1} cm^{-1} at 495 nm for fluorescein. Protein concentration was determined by the method of Lowry et al. (14a).

Cells and Microinjection: Human foreskin fibroblasts, type 356, were obtained from Dr. R. DeMars, Department of Genetics, University of Wisconsin, and cultured in Ham's F-10 medium supplemented with 10% fetal bovine serum. Cells were transferred to and microinjected in Leibovitz's medium (L-15) supplemented with 10 mM HEPES, pH 7.5 and 10% fetal bovine serum. DTAF–tubulin was microinjected at 4 mg/ml in 100 mM PIPES, 0.1 mM $MgCl_2$, and 1 mM GTP. Microinjection was performed with back-loaded glass capillaries by using a Leitz micromanipulator (E. Leitz, Inc., Rockleigh, NJ) and a Nikon inverted microscope (Nikon, Inc., Garden City, NY), according to the general procedures reviewed by Kreis and Birchmeier (15). With these procedures, the injected volume may vary from 1 to 10% of the cell volume, and for the purpose of calculations, was estimated at 5%.

Three criteria were used to assess that neither the injection buffer nor the injection procedure caused evident injury to the cells: (*a*) cell morphology and the microtubule network as determined by immunofluorescence were not detectably altered; (*b*) microinjected cells that were cold treated at 4°C for 30 min, then re-warmed to 37°C, re-formed normal microtubule networks; and (*c*) mitotic cells injected in prophase, metaphase, or anaphase progressed through mitosis. Qualitatively similar patterns of DTAF–tubulin incorporation were observed over the range of temperatures, 25–37°C, and in the rat kangaroo epithelial cell line, PtK_1.

At given time points after microinjection, cells were rinsed briefly in PEM buffer (100 mM PIPES, 10 mM EGTA, 2 mM $MgCl_2$, pH 6.94), extracted for 1 min in 0.1% Triton X-100 in PEM supplemented with 10 μg/ml taxol (National Cancer Institute, Bethesda, MD), fixed for 2 min with 0.5% glutaraldehyde in PEM, then treated with 2 mg/ml $NaBH_4$ in H_2O for 5 min to quench residual glutaraldehyde. The extraction procedure was used to remove DTAF–tubulin not incorporated into microtubules (10). Taxol was included to stabilize microtubules during extraction. Controls in which cells were not stabilized with taxol but rather were fixed and extracted simultaneously gave similar results but with a higher background, presumably because of the soluble, nonextracted DTAF–tubulin.

Immunofluorescence: Double-label immunofluorescence was performed sequentially to completely avoid bleed-through of rhodamine tubulin staining into the fluorescein DTAF–tubulin channel. DTAF–tubulin was stained and photographed first; then cells were stained for anti-tubulin immunofluorescence. DTAF–tubulin staining was done as follows: Antiserum to the fluorescein hapten was elicited by immunization of rabbits with fluoresceinated keyhole limpet hemocyanin as described (16). Cells were reacted with a 1:50 dilution of the rabbit antiserum in 20% normal goat serum in phosphate-buffered saline (PBS); (150 mM NaCl, 10 mM NaH_2PO_4, pH 7.6) for 30 min at 37°C. The secondary antibody was a 1:30 dilution of fluorescein-conjugated goat anti-rabbit IgG (Cappel Laboratories, Inc., Malvern, PA) in 10% normal goat serum in PBS for 30 min at 37°C. Tubulin staining was done as follows: Cells were reacted with a 1:1,000 dilution of an ascitic fluid of the YL ½ rat monoclonal antibody to yeast tubulin (gift of Dr. J. V. Kilmartin, Medical Research Council, England) in 10% bovine serum albumin in PBS for 30 min at 37°C. The secondary antibody was a 1:30 dilution of rhodamine-conjugated goat anti-rat IgG (Cappel Laboratories, Inc.) in PBS for 30 min at 37°C. Coverslips were mounted in 2% *N*-propyl gallate in 90% glycerol, pH 8.0 (17), examined with a Zeiss Universal microscope (Carl Zeiss, Inc., Thornwood, NY) by use of a 63× planapochromat (1.4 numerical aperture), and photographed on Kodak Tri-X film, pushed 1 stop with Kodak HC-110 developer.

Microtubule Length Distributions: Immunofluorescence micrographs were enlarged photographically, and microtubules were traced manually onto clear acetate. Lengths of individual microtubules were then determined by use of the Distance subroutine of an Apple Graphics Tablet coupled to an Apple II plus microcomputer (Apple Computer, Inc., Cupertino, CA).

RESULTS

Fluorescein was used as the hapten (18) and tubulin was conjugated with DTAF. This conjugate has been used by others for the direct visualization of microinjected tubulin in living cells by use of fluorescence microscopy and video intensification (7, 8, 19, 20). We found the direct fluorescence emission of this fluorophore useful to identify injected cells and to observe generalized fibrous patterns, but the signal-to-noise ratio was too poor to record single microtubules in living cells. We improved the signal-to-noise ratio both by amplifying the signal and by reducing the noise level. Amplification of the fluorescence signal was achieved by indirect immunofluorescent staining for the haptenic group. Noise was reduced by extracting the cells before fixation to remove the DTAF–tubulin not incorporated into microtubules.

Briefly, our procedure was to lyse and fix cells at given times after microinjection. The cells were then stained with the antibody to the fluorescein moiety and a secondary antibody conjugated with fluorescein. The relationship between newly incorporated tubulin and preexisting microtubules was determined by the staining of cells with anti-tubulin and a secondary antibody conjugated with rhodamine. Newly formed microtubule domains, which contained DTAF–tubulin, would give a signal in the fluorescein channel and appear green. The total microtubule distribution (preexisting as well as newly formed microtubule domains) would give a signal in the rhodamine channel and appear red. If the DTAF–tubulin exchanged with subunits all along the length of microtubules, as was suggested by recent studies (7, 8), then all microtubule domains would label both green and red. If, however, addition of DTAF–tubulin was restricted to the ends of microtubules, then we would expect to see green and red label coincident only over domains at the ends of microtubules, with the remainder of the microtubule lengths appearing red only. Newly formed microtubules, however, would appear green and red along their entire length.

Over the course of these experiments, ~350 cells were microinjected. Of these, ~¾ were photographed in fluorescence microscopy, the others being either underinjected by volume (giving low fluorescence emission) or overinjected (generally did not survive long term) and therefore were disqualified. Of the photographed cells, most presented a fibrous pattern that was interpretable at the level of single microtubules at least in some, generally peripheral, regions of the cell. Principal variations in the pattern were in the length

[1] *Abbreviations used in this paper*: DMSO, dimethyl sulfoxide; DTAF, dichlorotriazinylaminofluorescein; PEM, a buffer that contains 100 mM PIPES, 10 mM EGTA, 2 mM $MgCl_2$, pH 6.94.

of labeled microtubules and in the number focusing at the centrosome.

Figs. 1 and 2 show the distribution of incorporated tubulin and total microtubules in cells 7 and 14 min, respectively, after microinjection. Parts (*a*) and (*b*) show the signals in the fluorescein and rhodamine channels, respectively, which even though are both white on black, will be referred to as green and red that represent DTAF-tubulin and total microtubules, respectively. Similar pairs of micrographs are presented in Figs. 3–8.

The first important result is that, at these early times after microinjection, only a small proportion of the total microtu-

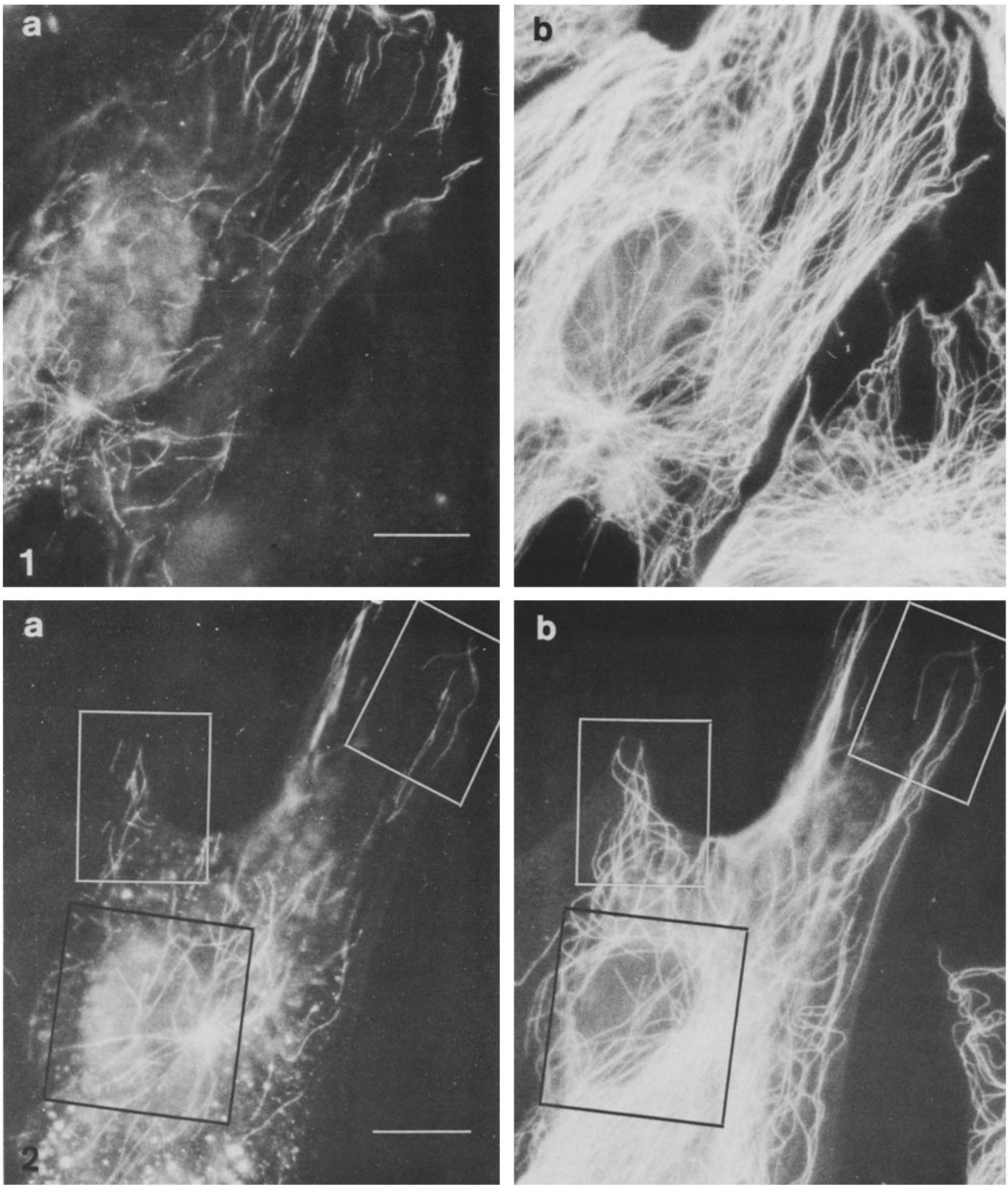

FIGURES 1 and 2 Double-label immunofluorescence of microinjected tubulin and the total microtubule profile. After microinjection of DTAF-tubulin, cells were lysed, fixed, and stained. (*a*) Fluorescein channel, antibody to DTAF-tubulin. (*b*) Rhodamine channel, antibody to tubulin. (Fig. 1) 7 min after microinjection. (Fig. 2) 14 min after microinjection. Three regions enclosed in Fig. 2 are shown in Figs. 5, 6, and 8. Bar in *a*, 10 μm. × 1,670.

bule profile was labeled green (had incorporated DTAF-tubulin). In the 7-min cell, most of the DTAF-tubulin was incorporated at the leading edge and was conspicuously absent from the side margins of the cell. Microtubules are known to end in the vicinity of the leading edge, and this pattern of labeling is consistent with incorporation at the ends of microtubules. In addition, a number of DTAF-microtubules were seen at the centrosome, which suggests that the centrosome had nucleated the formation of some new microtubules. However, most of the centrosomal microtubules were red but not green, which indicates that they had not incorporated label by this time. Finally, we noted the presence of short DTAF-tubulin segments scattered through the cytoplasm. These may have resulted from end addition to microtubules that did not extend to the edge of the cell or from new self-assembly in the cytoplasm. Because of the congestion of microtubules in this region, we could not distinguish between these alternatives in this cell. In the 14-min cell, prominent growth at the centrosome was observed, with some microtubules >10-μm long. However, as in the 7-min cell, the number of microtubules at the centrosome that incorporated DTAF-tubulin was significantly less than the total number of centrosomal microtubules.

In peripheral regions of cells, the relationship between the newly incorporated tubulin and the preexisting microtubules was more evident. Fig. 3 shows a striking example of a short bundle of intense green labeling at the end of a long, loosely organized bundle of microtubules, which suggests that assembly of the entire green bundle was seeded at its base. Despite the high number of microtubules in the bundle, virtually no incorporation of DTAF-tubulin along its length was observed. Presumably, this was due to the lack of microtubule ends except at the cell periphery. Another region at the edge of a cell (Fig. 4) shows microtubules running parallel to each other. Here, a one-to-one correspondence may be made between the green and red fibers. Every cellular microtubule in this field (red) was seen to have its distal tip green, which indicates that incorporation had occurred at the end. However, the congestion in the field was too great to permit tracking of the green domains proximally to determine if, in fact, they were co-linear with red fibers that extended toward the cell center.

In some regions of the cell periphery or over the nucleus, the sparsity of cellular microtubules permitted us to track individual microtubules along their length and to determine more precisely the domain of incorporation. Figs. 5–7 show three such regions with interpretative diagrams of the labeling patterns. Figs. 5 and 6 are higher magnification micrographs of two of the enclosed regions in the cell shown in Fig. 2. In each of these examples, most DTAF-labeled domains were identifiable as being co-linear with a microtubule and occurring at the end closest to the cell periphery. Fig. 6 also shows a rare example of a microtubule in which both ends may be seen. This apparently is a free cytoplasmic microtubule. Comparison of the fluorescein and rhodamine channels shows that the microtubule end closest to the cell periphery is red and green, whereas the opposite end is solely red. This is consistent with polar assembly onto a preexisting microtubule in vivo. No free microtubules labeled green and red along their entire length were observed, which suggests no self-assembly after the microinjection had occurred.

Fig. 8 is a high magnification micrograph of the nuclear region of the cell shown in Fig. 2 and shows microtubule growth from a centrosome. Approximately 15 microtubules, both green and red along their length, radiate from the centrosome, which is also the focus for perhaps a hundred microtubules that are red but not green. This suggests that the green and red microtubules were the result of new nucleation at the centrosome. The lengths of the green microtubules exceeded 10 μm and were comparable to the lengths of green domains seen at the periphery of the same cell.

Fig. 9 shows a quantitative analysis of the lengths of labeled microtubules at the periphery of a cell 9 min after microin-

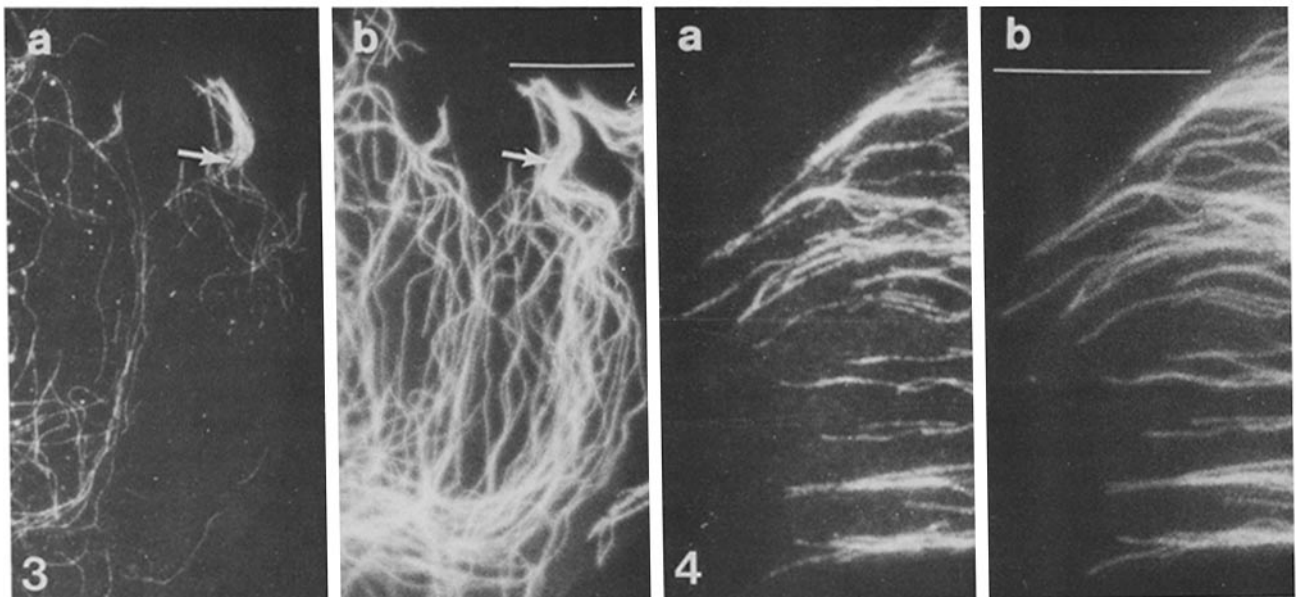

FIGURES 3 and 4 (Fig. 3) Distribution of DTAF-tubulin within a loosely organized microtubule bundle that extends upwards to the cell periphery. Cell 15 min after microinjection. (*a*) DTAF-tubulin microtubules; (*b*) total microtubules. Arrows mark the base of a peripheral bundle in *a* that appears seeded from preexisting microtubules. Bar in *b*, 10 μm. × 1,670. (Fig. 4) Correspondence between microtubule ends that incorporate DTAF-tubulin and total microtubule ends at a cell periphery. Cell 19 min after microinjection. (*a*) DTAF-tubulin microtubules; (*b*) total microtubules. Bar in *b*, 10 μm. × 2,840.

jection. Microtubules nucleated by the centrosome were not included in this analysis. The histogram shows a range of labeled lengths with a mean of 5.45 μm; maximum length was 15.5 μm. By assuming a uniform rate of incorporation after microinjection, we calculate that these lengths suggest an average elongation rate for microtubules in vivo of ~0.6

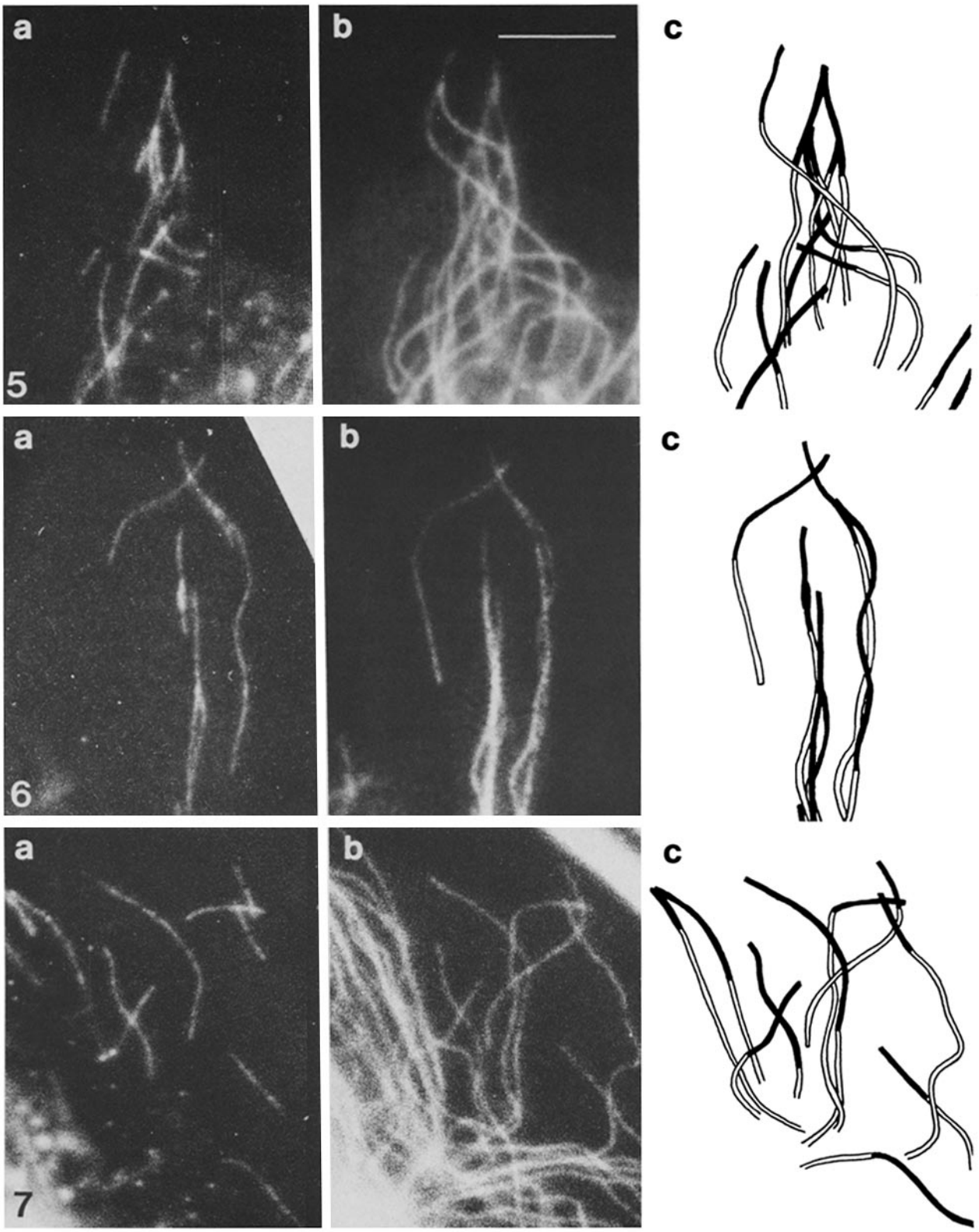

FIGURES 5–7 Distal incorporation of microinjected tubulin relative to preexisting microtubules. (*a*) DTAF-tubulin microtubules; (*b*) total microtubules; (*c*) interpretative diagrams that show end assembly of DTAF-tubulin (blackened segments) onto preexisting microtubules (open segments). In *c*, microtubules in *b* that do not show an end were omitted. Also, preexisting microtubules are incompletely depicted when pathways in *b* were uninterpretable. Figs. 5 and 6 are from two enclosed regions of the cell in Fig. 2 (14 min postinjection). Cell in Fig. 7 is 12 min after microinjection. Bar in 5*b*, 5 μm. × 4,000.

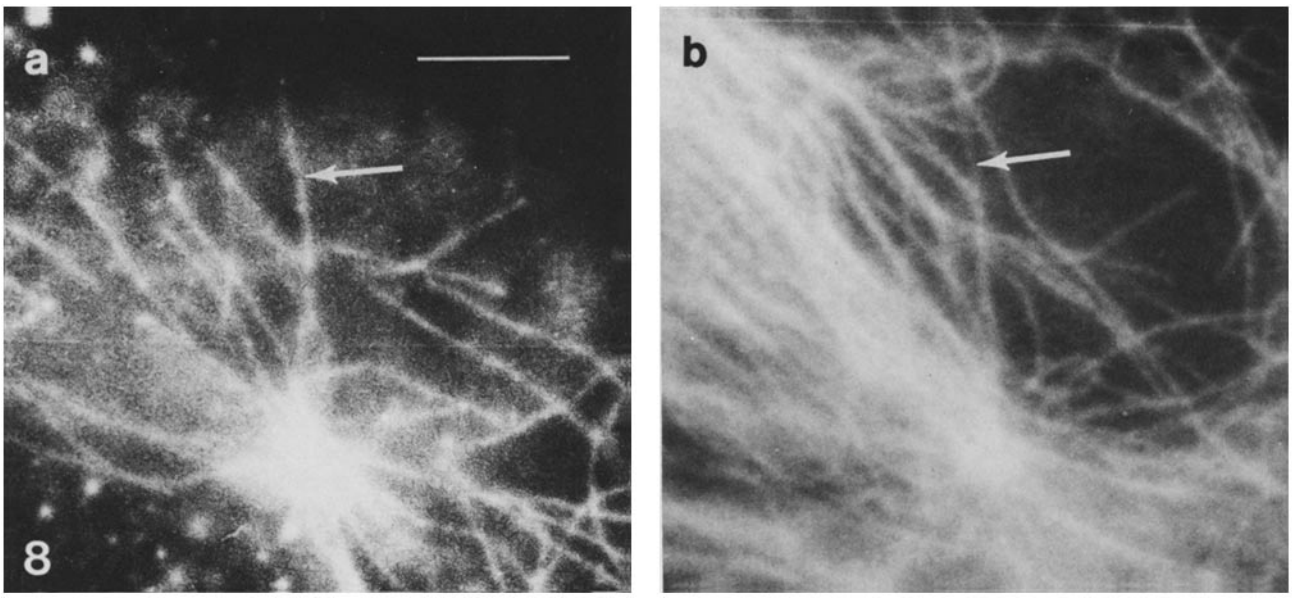

FIGURE 8 Centrosomal incorporation of DTAF-tubulin relative to total microtubules at the centrosome. (*a*) DTAF-tubulin microtubules; (*b*) total microtubules. One of the microtubules that originates at the centrosome in *a* and is identifiable in *b* is denoted with arrows. This figure is the enclosed nuclear region of the cell in Fig. 2. Bar, 5 μm. × 4,000.

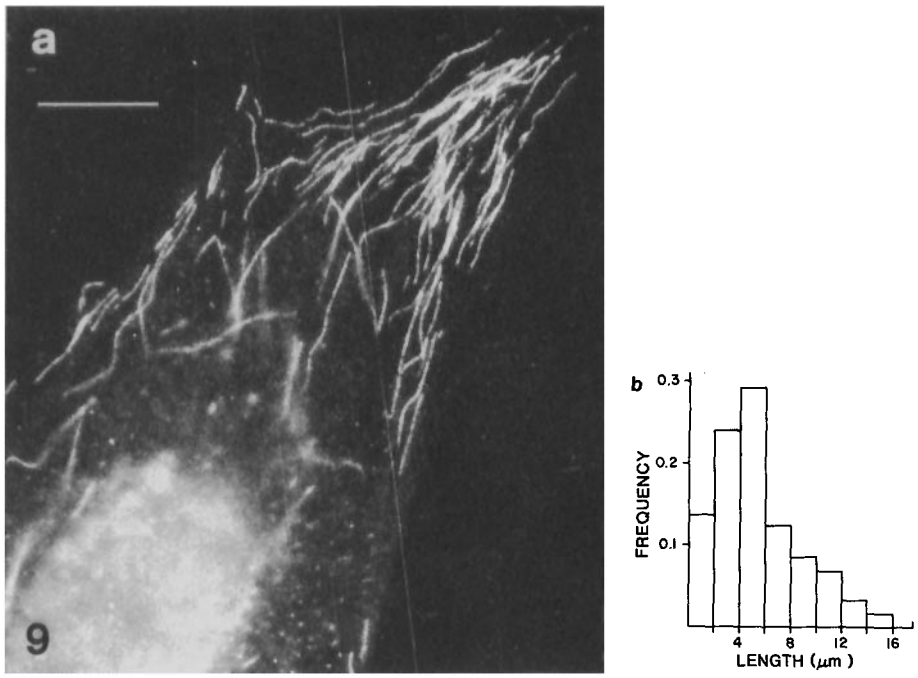

FIGURE 9 Microtubule length distributions of DTAF-tubulin in vivo. (*a*) DTAF-tubulin incorporation at the edge of a cell 9 min after microinjection. (*b*) Histogram of the lengths of 58 microtubule segments measured from *a* where two ends were clearly identifiable. Mean was 5.45 μm. Bar in *a*, 10 μm. × 1,600.

μm/min. Because we have not attempted to quantitate precisely the amount of DTAF-tubulin microinjected, rates of elongation as determined in different cells are not directly comparable.

DISCUSSION

The rationale behind our approach was to combine microinjection of haptenized tubulin and hapten-mediated immunocytochemistry (9, 10, 11) to determine directly the site and directionality of microtubule assembly in vivo. Hapten-mediated immunocytochemistry was essential to amplify signals sufficiently to permit the location of added tubulin subunits in individual microtubules. Fluorescein was a convenient hapten (18) and also allowed immediate confirmation by fluorescence microscopy of the microinjection.

Current understanding of microtubule polymerization in vitro indicates three classes of microtubule growth are possible in living cells: (*a*) elongation of preexisting microtubules by addition of subunits at their ends; (*b*) nucleation of microtubules by specialized structures such as the centrosome; and (*c*) self-assembly leading to the formation of free microtubules.

Our studies demonstrate clearly the incorporation in vivo of subunits at the distal ends of microtubules. Structural polarity studies (21, 22) have shown that microtubules in animal cells radiate from the centrosomal region with their plus ends distal. Thus, we can identify the distal labeling in

vivo as signifying incorporation at the plus end. Analysis of occasionally observed free microtubules also show incorporation only at one end, which indicates that growth is polar in vivo as it is in vitro (3). No newly self-assembled microtubules were observed, although their existence cannot be ruled out.

The second category of growth, nucleation by the centrosome, is also strongly indicated, although there is some difficulty in tracing labeled microtubules to their end points. The distal tip labeling described previously is presumably at the plus ends of preexisting centrosomal microtubules or other long microtubules that trace to the nuclear region. Interestingly, in every case when red microtubules could be traced to their distal tips, their ends were observed to be green, which indicates that none of the preexisting microtubules was incapable of assembly or "capped" at its plus ends. Such microtubules may exist, but we have found none under our experimental conditions. In contrast, at early times after microinjection, most microtubules at the centrosome were unlabeled. This indicates that most microtubules at the centrosome do not incorporate subunits at their minus end, and, therefore, are "capped." We conclude that the centrosomal microtubules labeled along their length represent newly formed microtubules, which grow by addition of subunits at their plus ends.

What does growth of new microtubules from the centrosome indicate? It could indicate that, in interphase cells, the centrosome is normally not saturated in terms of its nucleating capacity. Microinjection of tubulin might have shifted the subunit/polymer ratio sufficiently away from steady-state to drive the formation of microtubules onto unoccupied nucleation sites, which leads to an increase in the number of centrosomal microtubules. A second possibility is predicted by the recently proposed model of dynamic instability (4). The new microtubules may represent nucleation at sites where microtubules have recently disappeared. Thus, the net number of microtubules would remain unchanged, and the rate of appearance of new microtubules would then indicate the steady-state rate of turnover of the microtubule population.

Microinjection of labeled tubulin and observation of incorporation at times after injection is by nature a perturbation-relaxation experiment. How significant might this perturbation be? Based on the concentration of the microinjected tubulin (4 mg/ml), the injected volume (~5%), and the concentration of cellular tubulin in subunit form (1.3 mg/ml) (23), we calculate that microinjection would elevate the subunit pool by ~15%. The observation that free microtubules grew only at one end suggests that the increase in concentration of free subunits was less than that necessary to cause minus end growth. Therefore, the results indicate that the concentration of free subunits initially after microinjection (~1.5 mg/ml) lay between the steady-state value and the critical concentration at the minus end.

The period of microtubule growth and subunit depletion to the steady-state level would constitute the relaxation phase. Based on kinetic parameters determined in vitro (1, 3), estimates of microtubule numbers in vivo (23), and a reversible equilibrium model,[2] we estimate the half-time for relaxation to be ~16 min, similar to the time scale of our experiments. Thus, the distal tip labeling observed may be accounted for simply in terms of subunit addition when the subunit concentration is above its equilibrium value. The observations do not exclude treadmilling, although other studies (8, 24) indicate that this process in interphase mammalian cells, if it occurs at all, is slow. If treadmilling occurred, we would expect the labeled zone to increase in length linearly with time, whereas if the mechanism of tip labeling were solely equilibrium perturbation, the length would increase asymptotically to a value equal to the proportion of total microtubule length represented by the injection tubulin.

It is useful to estimate the sensitivity of our detection system for incorporation of DTAF-tubulin. Based on a fluorochrome-to-tubulin ratio for the DTAF-tubulin of 0.5, the estimated concentration of microinjected tubulin of 0.2 mg/ml, and the estimated concentration of cellular tubulin in subunit form of 1.3 mg/ml, we may calculate the proportion of labeled subunits in the cellular pool after microinjection to be 1 in 15. By assuming that labeled and unlabeled tubulin incorporate into microtubules equally and that there are 1,625 subunits/μm of microtubule, we calculate that this value corresponds to 108 labeled subunits/μm. We have not yet determined precisely our threshold for detection, but we estimate it to be ~fivefold lower or ~20 labeled subunits/μm.

In summary, our studies demonstrate that the sites of microtubule assembly in interphase mammalian cells are at the plus ends of preexisting microtubules and at centrosomes. These are both end-dependent mechanisms and are fully consistent with in vitro results. However, our results do not distinguish among the possible end-dependent mechanisms of assembly: equilibrium perturbation, treadmilling, and dynamic instability. Now that it is possible to study the activity of individual microtubules in cells, we expect kinetic analyses to resolve the open issues in vivo as they have in vitro.

We thank Gary Gorbsky for the antiserum to fluorescein and John Peloquin for technical assistance, criticism, and help with the manuscript. We also thank Bob Silver, Paul Sammak, Dale Vandre, Dan Webster, Soo-Siang Lim, and Gordy Hering for comments on the manuscript.

This work was supported by National Institutes of Health grant GM 25062.

Received for publication 10 January 1985, and in revised form 7 February 1985.

REFERENCES

1. Johnson, K. A., and G. G. Borisy. 1977. Kinetic analysis of microtubule assembly *in vitro*. *J. Mol. Biol.* 117:1–31.
2. Margolis, R. L., and L. Wilson. 1978. Opposite end assembly and disassembly of microtubules at steady-state *in vitro*. *Cell.* 13:1–8.
3. Bergen, L. G., and G. G. Borisy. 1980. Head-to-tail polymerization of microtubules in vitro: electron microscope analysis of seeded assembly. *J. Cell Biol.* 84:141–150.
4. Mitchison, T., and M. Kirschner. 1984. Dynamic instability of microtubule growth. *Nature (Lond.).* 312:237–242.
5. Inoué, S. 1964. Organization and function of the mitotic spindle. *In* Primitive Motile Systems in Cell Biology. R. D. Allen, editor. Academic Press, Inc., New York. 549–594.
6. Inoué, S., and H. Ritter. 1975. Dynamics of mitotic spindle organization and function. *In* Molecules and Cell Movement. S. Inoué and R. E. Stephens, editors. Raven Press, New York. 3–29.
7. Salmon, E. D., R. J. Leslie, W. M. Saxton, M. L. Karow, and J. R. McIntosh. 1984. Spindle microtubule dynamics in sea urchin embryos: analysis using a fluorescein-

[2] The kinetics of assembly of microinjected tubulin can be analyzed on an equilibrium perturbation model as a pseudo-first order reaction in which the time required to complete half the reaction, $t_{1/2}$, is given by $t_{1/2} = \ln 2/k_+ [M]$, where k_+ is the association rate constant for the plus end, and [M] is the molar concentration of microtubule ends. [M] was calculated from the estimated number of microtubules per cell, 150, and the average cell volume, 2.6×10^{-12} liters, for 3T3 cells (23) and from Avogadros number, 6×10^{23}, to be $\sim 1 \times 10^{-10}$ M. By taking a value for k_+ of 7.2×10^6 $M^{-1}s^{-1}$ (3), we calculate $t_{1/2}$ to be 16 min.

labeled tubulin and measurements of fluorescence redistribution after laser photobleaching. *J. Cell Biol.* 99:2165–2174.
8. Saxton, W. M., D. L. Stemple, R. J. Leslie, E. D. Salmon, M. Zavortink, and J. R. McIntosh. 1984. Tubulin dynamics in cultured mammalian cells. *J. Cell Biol.* 99:2175–2186.
9. Soltys, B. J., G. Gorbsky, and G. G. Borisy. 1983. Immunoelectron microscopy of hapten-conjugated microtubules and F-actin in vitro and in microinjected fibroblasts. *J. Cell Biol.* 97(5, Pt. 2):374*a*. (Abstr.)
10. Soltys, B. J., and G. G. Borisy. 1984. Correlative light and electron microscopy of microinjected fluorescent tubulin or actin. *J. Cell Biol.* 99(4, Pt. 2):196*a*. (Abstr.)
11. Luby-Phelps, K., P. A. Amato, and D. L. Taylor. 1984. Selective immunocytochemical detection of fluorescent analogs with antibodies specific for the fluorophore. *Cell Motil.* 4:137–149.
12. Borisy, G. G., J. M. Marcum, J. B. Olmsted, D. B. Murphy and K. A. Johnson. 1975. Purification of tubulin and associated high molecular weight proteins from porcine brain and characterization of microtubule assembly *in vitro*. *Ann. NY Acad. Sci.* 253:107–132.
13. Vallee, R. B., and G. G. Borisy. 1978. The non-tubulin component of microtubule protein oligomers. *J. Biol. Chem.* 253:2834–2845.
14. Blakeslee, D. 1977. Immunofluorescence using dichlorotriazinylaminofluorescein (DTAF). II. Preparation and stability of the compound. *J. Immunol. Methods.* 17:361–364.
14a. Lowry, O. H., N. J. Rosebrough, A. L. Farr, and R. J. Randall. 1951. Protein measurement with the Folin-phenol reagent. *J. Biol. Chem.* 193:265–275.
15. Kreis, T. E., and W. Birchmeier. 1982. Microinjection of fluorescently labeled proteins into living cells with emphasis on cytoskeletal proteins. *Int. Rev. Cytol.* 75:209–227.
16. Gollogly, J. R., and R. E. Cathou. 1974. Sequential appearance of three different anti-fluorescein combining sites in hyperimmunized rabbits. Characterization by circular dichoism and binding studies. *J. Immunol.* 113:1457–1468.
17. Giloh, H., and J. W. Sedat. 1982. Fluorescence microscopy: reduced photobleaching of rhodamine and fluorescein protein conjugates by *n*-propyl gallate. *Science (Wash. DC).* 217:1252–1255.
18. Voss, E. W. 1984. Fluorescein hapten: an immunological probe. CRC Press, Inc., Boca Raton, Florida. 193 pp.
19. Keith, C. H., J. R. Feramisco, and M. Shelanski. 1981. Direct visualization of fluorescein-labeled microtubules *in vitro* and in microinjected fibroblasts. *J. Cell Biol.* 88:234–240.
20. Wadsworth, P., and R. D. Sloboda. 1983. Microinjection of fluorescent tubulin into dividing sea urchin cells. *J. Cell Biol.* 97:1249–1254.
21. Euteneuer, V., and J. R. McIntosh. 1981. Polarity of some motility-related microtubules. *Proc. Natl. Acad. Sci. USA.* 78:372–376.
22. Telzer, B. R., and L. T. Haimo. 1981. Decoration of spindle microtubules with dynein: evidence for uniform polarity. *J. Cell Biol.* 89:373–378.
23. Hiller, G., and K. Weber. 1978. Radioimmunoassay for tubulin: a quantitative comparison of the tubulin content of different established tissue culture cells and tissues. *Cell.* 14:795–804.
24. Scherson, T., T. E. Kreis, J. Schlessinger, U. Z. Littauer, G. G. Borisy, and B. Geiger. 1984. Dynamic interactions of fluorescently labeled microtubule-associated proteins in living cells. *J. Cell Biol.* 99:425–434.